AFRL-VA-WP-TP-2006-335

APPLICATION OF A SPECTROSCOPIC MEASURING TECHNIQUE TO PLASMA DISCHARGE IN HYPERSONIC FLOW (POSTPRINT)

Scott A. Stanfield, James Menart, Joseph Shang, Roger L. Kimmel, and James R. Hayes

JANUARY 2006

Approved for public release; distribution is unlimited.

STINFO COPY

AIR VEHICLES DIRECTORATE
AIR FORCE MATERIEL COMMAND
AIR FORCE RESEARCH LABORATORY
WRIGHT-PATTERSON AIR FORCE BASE, OH 45433-7542

NOTICE AND SIGNATURE PAGE

AFRL-VA-WP-TP-2006-335 HAS BEEN REVIEWED AND IS APPROVED FOR PUBLICATION IN ACCORDANCE WITH ASSIGNED DISTRIBUTION STATEMENT.

*//Signature//	//Signature//
Roger L. Kimmel	Carl Tilmann
Senior Research Engineer	Acting Chief
Aeroconfiguration Research Branch	Aeroconfiguration Research Branch

*Disseminated copies will show "//signature//" stamped or typed above the signature blocks.

REPORT DOCUMENTATION PAGE

Form Approved
OMB No. 0704-0188

1. REPORT DATE *(DD-MM-YY)*	2. REPORT TYPE	3. DATES COVERED *(From - To)*
January 2006	Conference Paper Postprint	01/01/2001 – 01/01/2006

4. TITLE AND SUBTITLE

APPLICATION OF SPECTROSCOPIC MEASURING TECHNIQUE TO PLASMA DISCHARGE IN HYPERSONIC FLOW (POSTPRINT)

5a. CONTRACT NUMBER
In-house

5b. GRANT NUMBER

5c. PROGRAM ELEMENT NUMBER
61102F

6. AUTHOR(S)

Scott A. Stanfield, James Menart, and Joseph Shang (Wright State University)
Roger L. Kimmel and James R. Hayes (AFRL/VAAA)

5d. PROJECT NUMBER
A03U

5e. TASK NUMBER

5f. WORK UNIT NUMBER
0B

7. PERFORMING ORGANIZATION NAME(S) AND ADDRESS(ES)

Wright State University
Dayton, OH 45435

Aerodynamic Configuration Branch (AFRL/VAAA)
Aeronautical Sciences Division
Air Vehicles Directorate
Air Force Materiel Command, Air Force Research Laboratory
Wright-Patterson Air Force Base, OH 45433-7542

8. PERFORMING ORGANIZATION REPORT NUMBER
AFRL-VA-WP-TP-2006-335

9. SPONSORING/MONITORING AGENCY NAME(S) AND ADDRESS(ES)

Air Vehicles Directorate
Air Force Research Laboratory
Air Force Materiel Command
Wright-Patterson Air Force Base, OH 45433-7542

10. SPONSORING/MONITORING AGENCY ACRONYM(S)
AFRL-VA-WP

11. SPONSORING/MONITORING AGENCY REPORT NUMBER(S)
AFRL-VA-WP-TP-2006-335

12. DISTRIBUTION/AVAILABILITY STATEMENT
Approved for public release; distribution is unlimited.

13. SUPPLEMENTARY NOTES

The U.S. Government is joint author of the work and has the right to use, modify, reproduce, release, perform, display, or disclose the work.

Conference paper published in the Proceedings of the 2006 44th AIAA Aerospace Sciences Meeting and Exhibit, published by AIAA. PAO Case Number: AFRL/WS 05-2811 (cleared 21 Dec 2005). Paper contains color.

14. ABSTRACT

Spatially resolved rotational temperatures have been obtained within the boundary layer of a flat plate model in a Mach 5.1 flow using emission spectroscopy. The temperatures were obtained by matching the measured nitrogen second positive 0-2 rovibrational band with a calculated one. Temperature profiles are given above the cathode and the anode. The maximum temperature obtained above the cathode did not correspond to the surface of the model, but rather at an elevation 0.55 mm above the surface. This indicates that heat is traveling from the discharge into the plate for a period of time after the discharge is ignited. This characteristic in the temperature profile sheds light on some of the effects a plasma has on the flow field as determined by Pitot probe measurements and total lift measurements.

15. SUBJECT TERMS

16. SECURITY CLASSIFICATION OF:			17. LIMITATION OF ABSTRACT:	18. NUMBER OF PAGES	19a. NAME OF RESPONSIBLE PERSON (Monitor)
a. REPORT	b. ABSTRACT	c. THIS PAGE			Roger L. Kimmel
Unclassified	Unclassified	Unclassified	SAR	18	19b. TELEPHONE NUMBER *(Include Area Code)* N/A

Standard Form 298 (Rev. 8-98)
Prescribed by ANSI Std. Z39-18

44th AIAA Aerospace Sciences Meeting and Exhibit
January 9 – 12, 2005, Reno, Nevada
AIAA 2006-0559

Application of a Spectroscopic Measuring Technique to Plasma Discharge in Hypersonic Flow

Scott A. Stanfield[*], James Menart[†], Joseph Shang[‡]
Wright State University, Dayton, Ohio, 45435

Roger L. Kimmel[§] and James R. Hayes[**]
Air Force Research Laboratory, Wright-Patterson AFB, Dayton, Ohio, 45433

Spatially resolved rotational temperatures have been obtained within the boundary layer of a flat plate model in a Mach 5.1 flow using emission spectroscopy. The temperatures were obtained by matching the measured nitrogen second positive 0-2 rovibrational band with a calculated one. Temperature profiles are given above the cathode and the anode. The maximum temperature obtained above the cathode did not correspond to the surface of the model, but rather at an elevation 0.55 mm above the surface. This indicates that heat is traveling from the discharge into the plate for a period of time after the discharge is ignited. This characteristic in the temperature profile sheds light on some of the effects a plasma has on the flow field as determined by pitot probe measurements and total lift measurements.

Nomenclature

$A_{v'}^{v''}$	=	Einstein coefficient
c	=	speed of light
d	=	distance between grooves on grating
f	=	focal length
$F_{J'}$	=	rotational energy of the upper state
h	=	Planck's constant
$I_{v'J'}^{v''J''}$	=	intensity of rovibrational line
k	=	Boltzmann's constant
m	=	diffraction order
n	=	number of pixels away from center pixel
$N_{v'}$	=	population of molecules in upper vibrational level
$P(\lambda,\lambda')$	=	instrumental line shape function of spectrometer
Q_r	=	rotational partition function
$S_J^{J''}$	=	rotational line strength
T	=	temperature

[*] PhD Candidate, Department of Mechanical and Materials Engineering, Stanfield.3@wright.edu, Member AIAA.
[†] Associate Professor, Department of Mechanical and Materials Engineering, james.menart@wright.edu, Member AIAA.
[‡]Research Professor, Department of Mechanical and Materials Engineering, joseph.shang@wright.edu, Fellow AIAA.
[§] Senior Research Engineer, Associate Fellow AIAA.
[**] Senior Research Engineer.

$W_{v'}^{v''}(\lambda)$ = measured intensity
x = pixel width
γ = inclusion angle or half angle
δ = detector angle
$\lambda_{v'J'}^{v''J''}$ = wavelength of the transition
ξ = angle incident ray strikes center pixel of CCD array
ψ = rotating angle of grating

I. Introduction

POSSIBLE benefits of magneto-aerodynamics, which are of great interest to the aerospace community include plasma flow control with applications to boundary layer transition control,[1] shock boundary layer interaction control, [2–3] virtual flap actuators for aerodynamic control, [4] drag reduction in flight, [5,6] and steering of high-speed aircraft. [7] These benefits may be achievable by generating a plasma discharge and applying a magnetic field in high-speed flows; however, they cannot be realized fully until the properties of plasma located in high-speed flows are well characterized. At the present time the combination of both Joule heating effects and heating from the electrode surface through convection have shown to noticeably alter the bulk of the fluid flow and alterations due to a Lorentzian force are not discernable. [8–9] This has led to the work being presented in this paper which is the characterization of the temperature profiles present in the boundary layer. This is done by spatially resolving rotational temperatures at different positions within the boundary layer using emission spectroscopy.

Hypersonic flow characteristics above the flat plate change significantly due to heating caused from igniting a plasma. These changes are understood by measuring the thermal boundary layer. There are a limited number of techniques capable of performing these measurements in nonequilibrium plasmas. One technique is to insert a temperature probe into the discharge. This method, which measures the recovery temperature, is intrusive and will not provide accurate measurements if it provides results at all because a probe such as a thermocouple interacts with the self induced electric field of the discharge. Also temperatures measured with a thermocouple will be skewed hotter than what is physically possible due to electrons condensing on the probe surface. These limitations with an intrusive temperature measurement demonstrate the need for a nonintrusive technique, such as spectroscopy. A spectroscopic method used for many nonequilibrium plasmas is rotational spectroscopy. Many times the rotational temperature and the translational temperature in a plasma are close to being equal. However, to measure rotational temperatures spectroscopically the rotational modes do not have to be in equilibrium with the translational, vibrational and electronic modes, the rotational modes only need to be in self equilibrium. If this is true then the rotational temperature can be found for complicated band structures by matching a calculated spectrum with the measured spectrum.[10-12] Another technique is the Boltzmann plot method.[13, 14]

II. Test Facilities and Equipment

Tests were conducted within a blow-down, free jet, Mach 5.1 flow channel located at Wright Patterson Air Force Base (see Fig. 1). The flow channel is constructed from acrylic plastic and assembled with nylon screws. The test section has a removable quartz cover plate to allow transmittance of radiation in the near infrared and visible wavelengths. The stagnation temperature is weakly dependent on the outdoor air temperature and is around 270K. The stagnation pressure has an operating range of 0.1 to 1.0 atm. More detail on the flow channel characteristics can be found in a prior publication. [15]

A flat plate model made out of a dielectric material with copper electrodes was used in this study. The cathode of the model was positioned up stream for every run. A schematic of the model is shown in Fig. 2.

The emitted radiation from the surface of the model is collected by a Newport KBX157 bi-convex lens with an effective focal length of 125 mm. The lens is positioned two times the focal length away from the discharge. A Newport aperture stop is used in front of the lens to help eliminate stray radiation. The image of the discharge is focused at a distance of two times the focal length of the collection lens onto a Roper Scientific LG-455-020-3 fiber

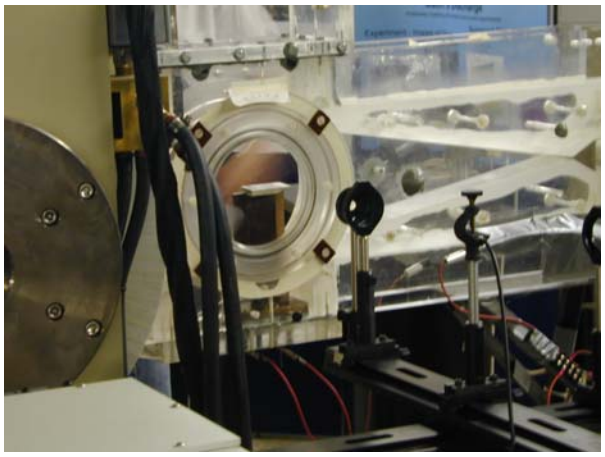

Figure 1. Photograph of test section in the Mach 5 flow channel and the optical setup.

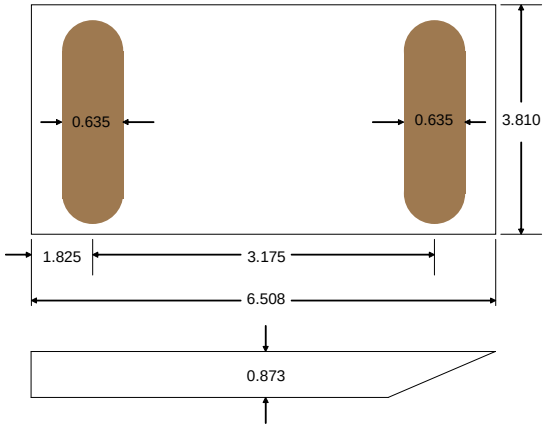

Figure 2. Model schematic. All dimensions are in cm.

optic bundle. The fiber optic bundle channels collected radiation from a spot size of 0.125 mm^2 into an Acton 2756 spectrometer where it is diffracted and focused onto an Andor DU 440-BU CCD camera. The spatial resolution of the measuring technique is given by the spot size divided by the magnification which is one for the lens used. The spatial resolution is 0.125 $mm.^2$ The spectrometer has a spectral resolution of 0.013 nm at 380.415 nm using a 3600 grooves per mm holographic grating blazed at 250 nm. The slit height and width respectively are 4 mm and 13μm. The optical components are mounted onto a rail positioned perpendicular (x-direction) to the flow through the wind tunnel. This rail is mounted onto another rail aligned in the flow direction (y-direction). This allows measurements to be taken at different positions in the y-direction. A scale is scribed onto the y-direction rail so that accurate positioning can be done in the flow direction. The y-direction rail is mounted to a steel elevating table. Measurements at different elevations in the discharge are obtained by raising and lowering the table. The table elevates by turning a wheel with diameter of 61.3 cm. Each complete turn of the wheel corresponds to a change in elevation of 8.3 mm. The wheel is divided into 61 even divisions where each division corresponds to a change in elevation of 0.14 mm. Fig. 3 shows the table along with the optics and how they are oriented with the test section. Alignment of the table with respect to the model was done using a large square. A level was used to adjust the table and model so that these surfaces are parallel.

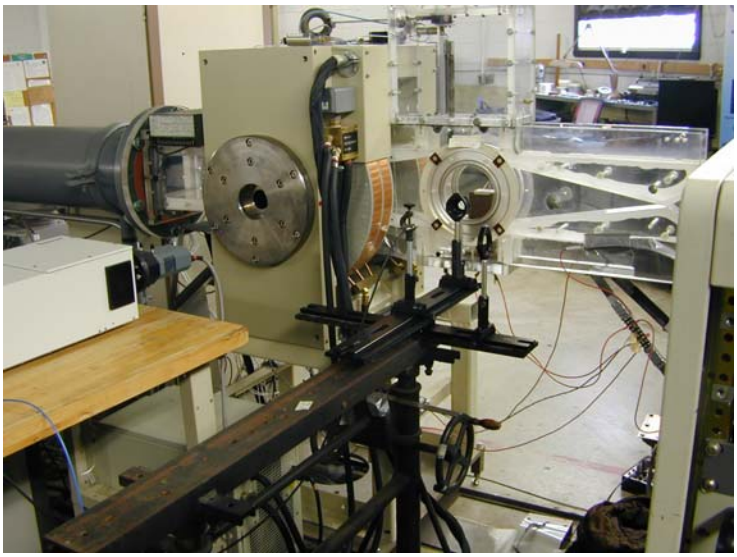

Figure 3. Photograph of the optical system, the table and the orientation of each piece with respect to the test section.

III. Rotational Temperature Determination

The rotational temperature was obtained by comparing the measured spectrum of the nitrogen second positive 0-2 transition to different theoretical spectrums calculated for different rotational temperatures.[10-12] The rotational temperature obtained corresponds to the calculated spectrum that best matches the experimental spectrum. This procedure is performed by a program called N2SPECFIT.[11]

Assuming an optically thin collection cone is used; the intensity of a rovibrational line can be written as[16]

$$I_{v'J'}^{v''J''} = \frac{N_{v'} A_{v'}^{v''}}{Q_r} S_J^{J''} e^{-F_{J'}/kT} \frac{hc}{\lambda_{v'J'}^{v''J''}} \quad . \tag{1}$$

The approximation to the measured spectrum is obtained from Eqn. (1) by summing up all the rovibrational lines and convolving them with the instrumental line shape function $P(\lambda, \lambda')$. The different broadening mechanisms of the measured spectrum produce half-widths that are at least an order of magnitude smaller than the half-width of the instrumental line function in the environment being investigated. Therefore the half-widths of the different broadening mechanisms present in the measured spectrum can be approximated by a Dirac delta function with minimal error. This assumption makes the convolution easier. The instrumental line shape function was obtained by measuring and curve fitting the spectra of a mercury discharge tube at 435.833 nm. This value, when convolved, may not broaden the calculated spectra enough to match the measured due to the assumption made with the broadening mechanisms. The variance of the calculated spectrum with respect to the measured spectrum can be improved by modifying the instrumental line function obtained. This produces negligible error. The calculated spectrum is then given by

$$W_{v'}^{v''}(\lambda) = \frac{N_{v'} A_{v'}^{v''}}{Q_r} hc \sum_{J'J''} S_{J'}^{J''} e^{-F_{J'}/kT_{rot}} \frac{P\left(\lambda, \lambda_{v'J'}^{v''J''}\right)}{\lambda_{v'J'}^{v''J''}} \quad . \tag{2}$$

The method described above to measure rotational temperatures assumes that the rotational temperature is uniform in the collection volume. This is clearly not the case in the current paper since the measurements were taken in a spatially non-uniform plasma. This error was reduced by minimizing the size of the collection volume. Also numerical verification was used to understand what temperature value would be obtained from a collection volume described by a range of rotational temperatures. This was done by generating different numerical spectra that contained equal weighted contributions from two temperatures and then using these spectra as inputs to the program

N2SPECFIT. The results are shown in Table 1 for seven different combinations of two temperature spectrums separated by 50 K. The tabulated values indicate that the software converges on a value around the average temperature of the combined temperature spectra. Therefore the rotational temperatures measured in this paper should be close to an average temperature over the spot size the radiation was collected from.

Temperature Mixture (K)	Converged Temperature Value (K)
450 and 400	423.9
400 and 350	373.9
350 and 300	323.8
300 and 250	273.7
250 and 200	223.5
200 and 150	172.8
150 and 100	120.7
100 and 50	78.5

Table 1. Converged temperatures found for different spectra mixtures.

IV. Experimental Procedures

A. Calibration

The wavelength falling onto the center pixel of the Andor CCD camera was calibrated using a helium discharge tube. The calibration of the Acton spectrometer assumes the wavelength focused onto the center pixel is dispersed linearly with the rotating grating. The software that operates the spectrometer takes the peak position of two different, single electronic transitions to calculate the offset and slope used for the calibration. The y-offset for the calibration was found using the helium line at 318.774 nm and the slope using the helium line at 447.147 nm. Several other electronic transitions were used to verify the calibration. The slope represents the rate of change of the wavelength over the angle of the grating. The calibration was off by five pixels in the spectral region of interest so the offset value was adjusted by this amount. The wavelength dispersion across the other pixels of the CCD camera was found using the grating equations. These equations assign a wavelength to each pixel and are dependent on the geometry of the spectrometer. The grating equations are given by

$$\lambda' = \frac{d}{m}\left\{\sin\left(\psi - \frac{\gamma}{2}\right) + \sin\left(\psi + \frac{\gamma}{2} + \xi\right)\right\} \tag{3}$$

$$\psi = \sin^{-1}\left(\frac{m\lambda_{CenterPixel}}{2d\cos\left(\gamma/2\right)}\right) \tag{4}$$

$$\xi = \tan^{-1}\left(\frac{nx\cos\delta}{f + nx\sin\delta}\right). \tag{5}$$

The response of the camera to a constant intensity source was not uniform across the CCD and was calibrated using a tungsten filament lamp with known spectral emission. This is a crucial step for properly measuring the intensity ratios of the different rotational transitions of a band which is necessary for obtaining accurate temperature measurements. Signal due to stray light inside the spectrometer caused from the imperfections of the mirrors used was accounted for by using a filter that blocks the wavelength range over which the calibration curve is being obtained. The calibration curve is given by

$$Calibration\ Curve(\lambda) = \frac{Tungsten\ Lamp\ Spectra(\lambda) - Stray\ Light\ Spectra(\lambda)}{Theoretical\ Tungsten\ Lamp\ Spectra(\lambda)}. \tag{6}$$

The calibrated data is given by

$$Calibrated\ Data(\lambda) = \frac{Raw\ Data(\lambda)}{Calibration\ Curve(\lambda)}\ . \tag{7}$$

B. Alignment and Preparation

Careful alignment of the table with respect to the model was performed. A large square was used to orient the table perpendicular to the model. A level was used to make sure both the model and table surfaces were horizontal. This is crucial and it was found by calculation that half a degree difference leads to significant error. The measurement volume of the optics inside the test section was found by shinning a laser through the back side of the fiber optical bundle. This technique was also used to locate the position of the leading edge of the model relative to the y-direction rail and this was taken as the position where y=0. The fiber optic cable was then carefully set back into its original position in the entrance slit of the spectrometer.

The camera was cooled to 218 K to reduce dark signal noise. All spectra scans were acquired with full vertical binning, 16 second pixel read out time, and background corrected spectra. The counts for each scan were held at a constant value just under saturation by increasing the exposure time. This means the overall exposure time was different for points measured at different positions in the discharge. Each scan was accumulated four times to increase the signal to noise ratio.

V. Results

Rotational temperatures were taken over the anode at a current of 25mA and over the cathode at 25mA and 50mA. The stagnation pressure was held at 370 torr for all cases and the stagnation temperatures varied between 274 K and 281 K. The profiles over the cathode are shown in Fig. 4. Points below an elevation of 0.3 mm include part of the model surface in the optical line of sight and the temperatures are skewed colder, possibly due to some reflected radiation off of the model surface. These points were omitted from the profiles and the first point taken corresponds to an optical line of sight free of the model surface. The first point of the 50mA case has a temperature of 360 K at an elevation of 0.3 mm and increases to a maximum value of 384 K at an elevation of 0.55 mm. The negative slope in the temperature profile at the model surface shows that heat is traveling into the cathode. The slopes $\frac{dT}{dy}$ at the cathode surface for the 25mA and 50mA cases are 108 and 165 K/mm respectively. Assuming the rotational temperature is in equilibrium with the translational temperature this is an important observation because it is a possible explanation for some transient behavior seen in pitot probe measurements[17] and total lift measurements[18] made in this facility. The assumption that translational energy modes are in equilibrium with the rotational modes stems from the small energy separation of a rotational transition which allows for rapid energy exchange between the two energy storage modes.[19]

Outside of the thermal boundary layer the temperature is measured to be 82 K. This temperature is higher than the analytically determined free stream static temperature downstream of the shock. The source of this error is not fully understood, but is believed to be caused by a combination of a weak signal in this region of the discharge and reflected radiation. The reflected radiation is believed to be coming from hotter portions of the discharge, thus raising the measured temperature.

The final interesting feature of the temperature profile is the change recorded across the shock. This change can be seen in Fig. 4 but it is easier to see in Fig. 5 which is an enlarged view of the shock region. The temperature drop calculated for an oblique shock with shock angle of 18.3^{o} and a Mach number of 5.1 is 18 K. The shock angle was obtained by using a protractor to measure the angle from a Schlieren image. The measured value found is only 7 K. The discrepancy is not fully understood but falls under the same explanation given for the skewed temperature values recorded in the free stream. The temperature jump across the shock is shown as having occurred over a 1.5 mm distance. This discrepancy is from both the spatial resolution of 0.125 mm^{2} and the accuracy of how level the optical system is to the model. Fig. 6 shows one of the measured radiation spectrums from this region overlaid with the calculated spectrum from N2SPECFIT. The calculated spectrum appears to agree well with the measured spectrum.

The rotational temperature profile for the anode is shown in Fig. 7. The glow over the anode is a lot smaller than that for the cathode. Because the discharge over the anode only emits significant radiation for a small height above the anode surface, measurements of the rotational temperature could only be made up to a location 3 mm above the surface. The portion of the temperature profile which could be obtained shows a constant temperature of about 299 K.

It is ideal to measure a single plasma temperature instead of an averaged value over a small collection volume. However, in our system there are three means by which a temperature gradient is present in the measurement. As mentioned before there is a gradient present at different elevations above the plate surface. The results in Fig. 4 show this. This occurs because a small but finite measurement size in the vertical direction is used. Another gradient exists in the spanwise direction of the discharge. The third temperature gradient is detected when the air heats up from the discharge over time during the accumulation process. This occurs from the electrodes heating up over time. The accumulation time used in this work varied depending on the location in the discharge. For locations close to the model surface short accumulation times varying from 6 to 12 seconds were used because the light intensity was strong. For locations away from the plate longer accumulation times up to 90 seconds were used because the intensity for the light signal was weak. From the results shown in Figs. 8 and 9 it can be seen that the large changes in temperatures with time occur close to the plate surface. Away from the surface the changes are much smaller. Figure 8 shows the results for temperature measurements taken over time in the free stream at an elevation of 4 mm. The maximum change in temperature is 2 K and corresponds to 50 mA of current with the discharge on for 40 seconds. The last point taken in Fig. 9 for the 50 mA case shows the temperature decreasing instead of increasing. This is due to the discharge breaking down. Figure 9 shows the temperature increasing as a function of time in the boundary layer. Notice that the temperature increase in the boundary layer is small for short time durations. Consequently the exposure times in the boundary layer where the signal is very strong were small and in the free stream where the signal was weak were long. Thus it is concluded that the variation of temperature with time is an unimportant effect in these measurements.

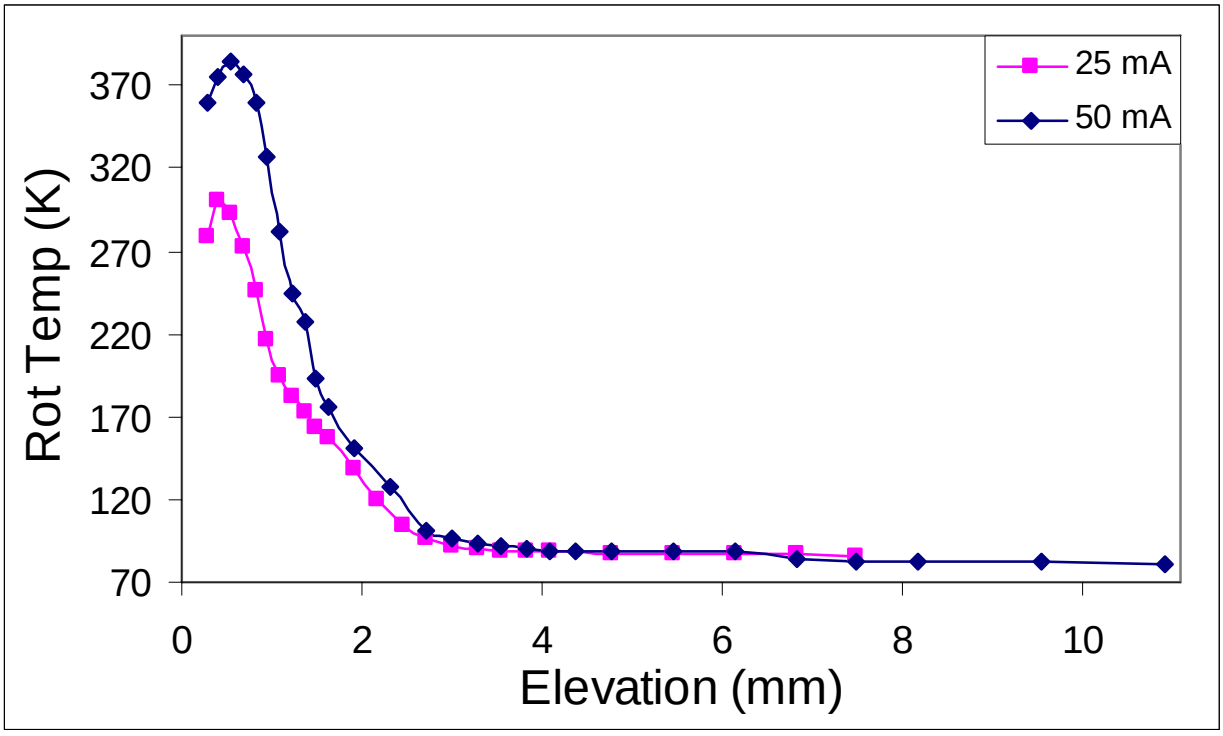

Figure 4. Rotational temperature profiles over the cathode at currents of 25 mA and 50 mA.

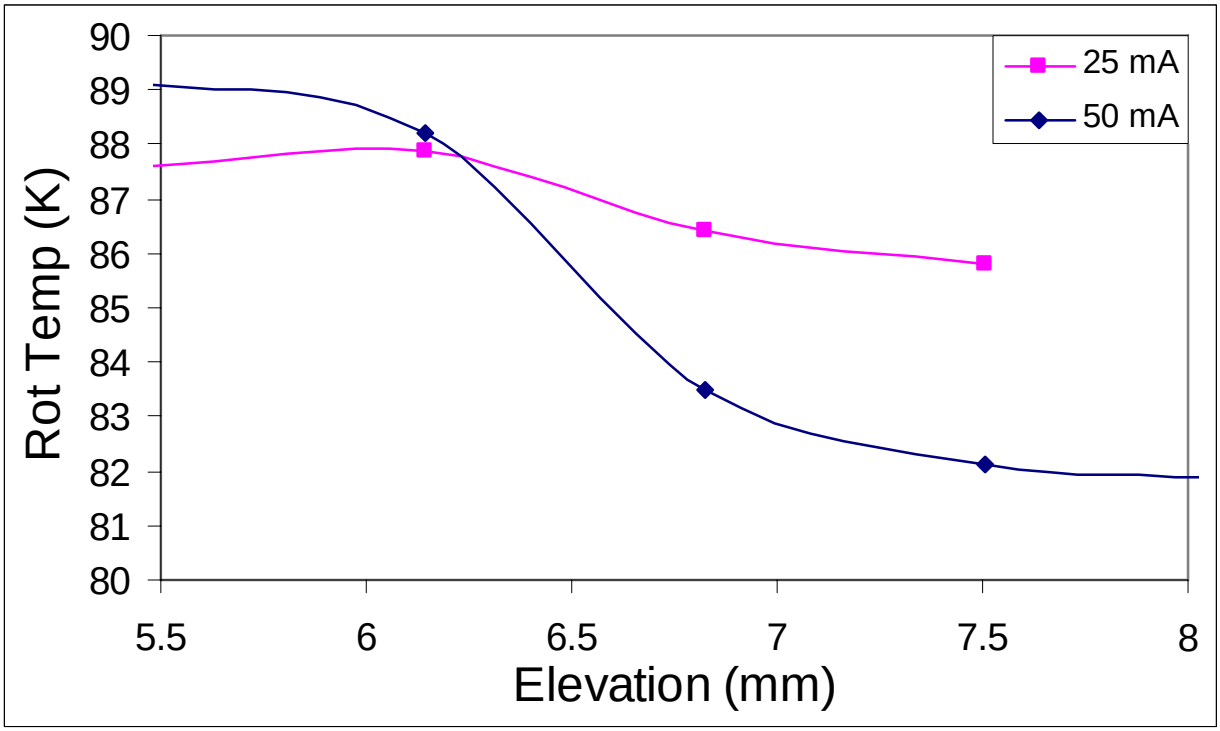

Figure 5. Close up of temperature jump across the shock from Fig. 4.

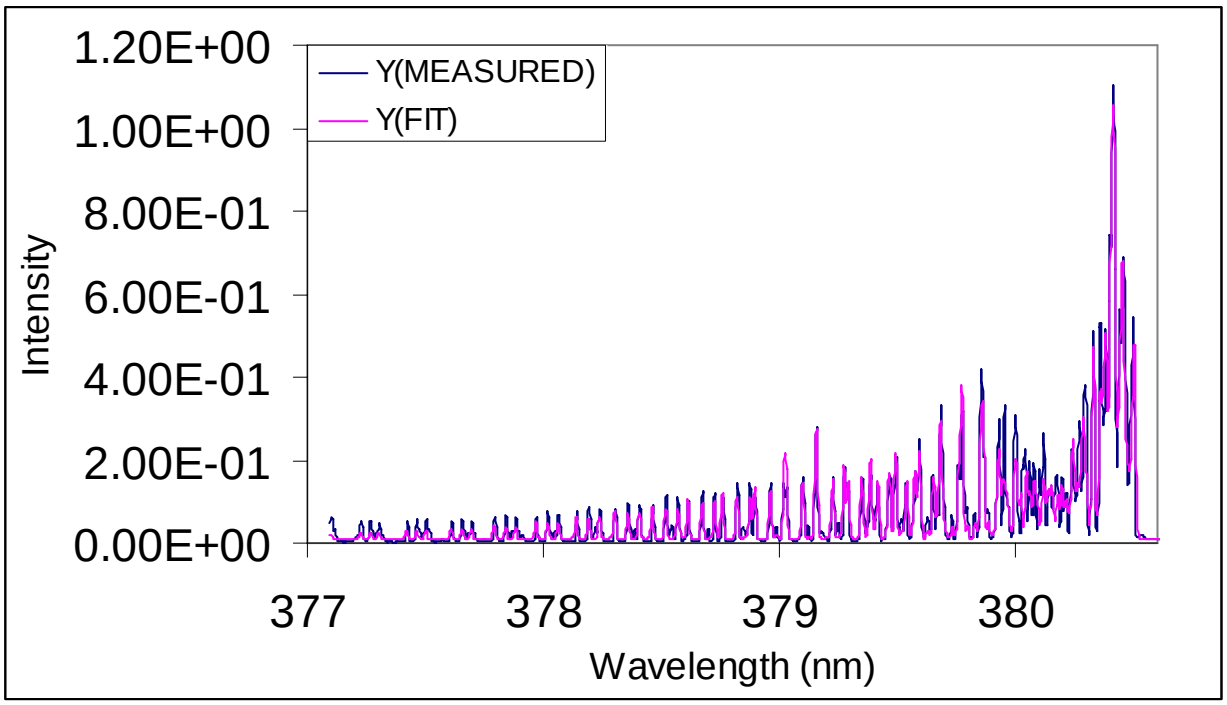

Figure 6. Output from N2SPECFIT shows a measure rovibrational band overlaid with the calculated fit.

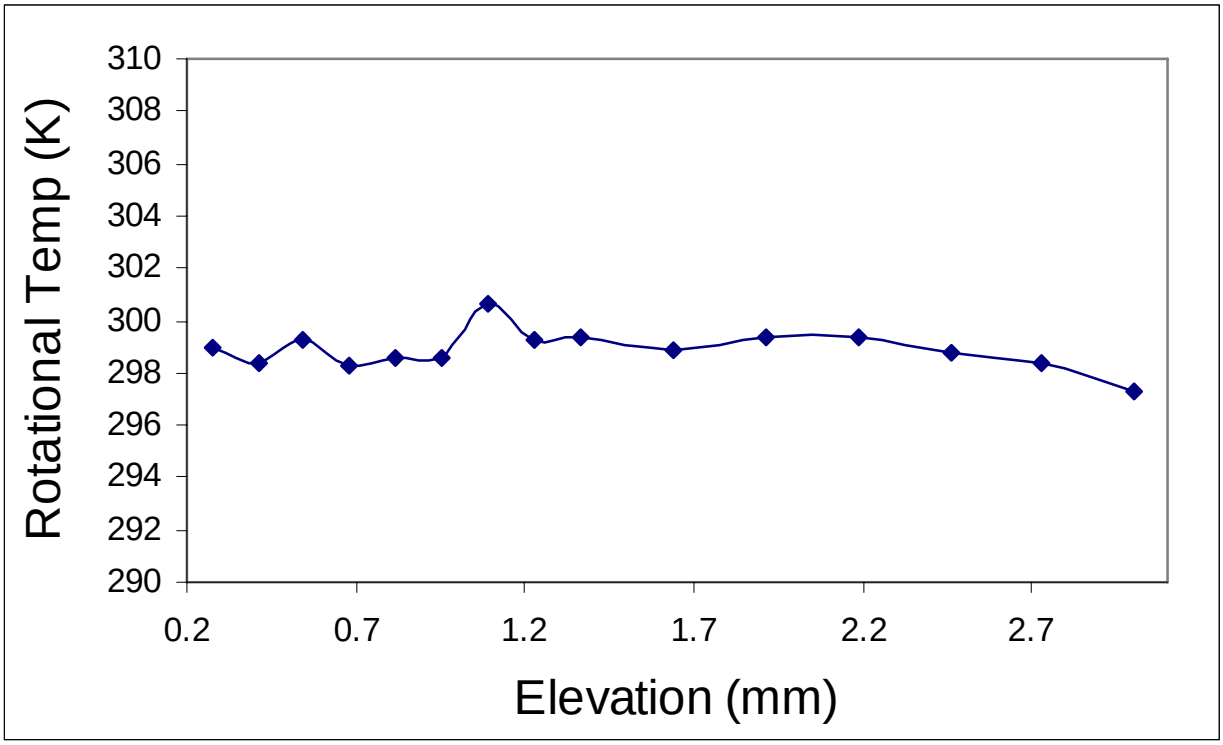

Figure 7. Rotational temperature profile over anode.

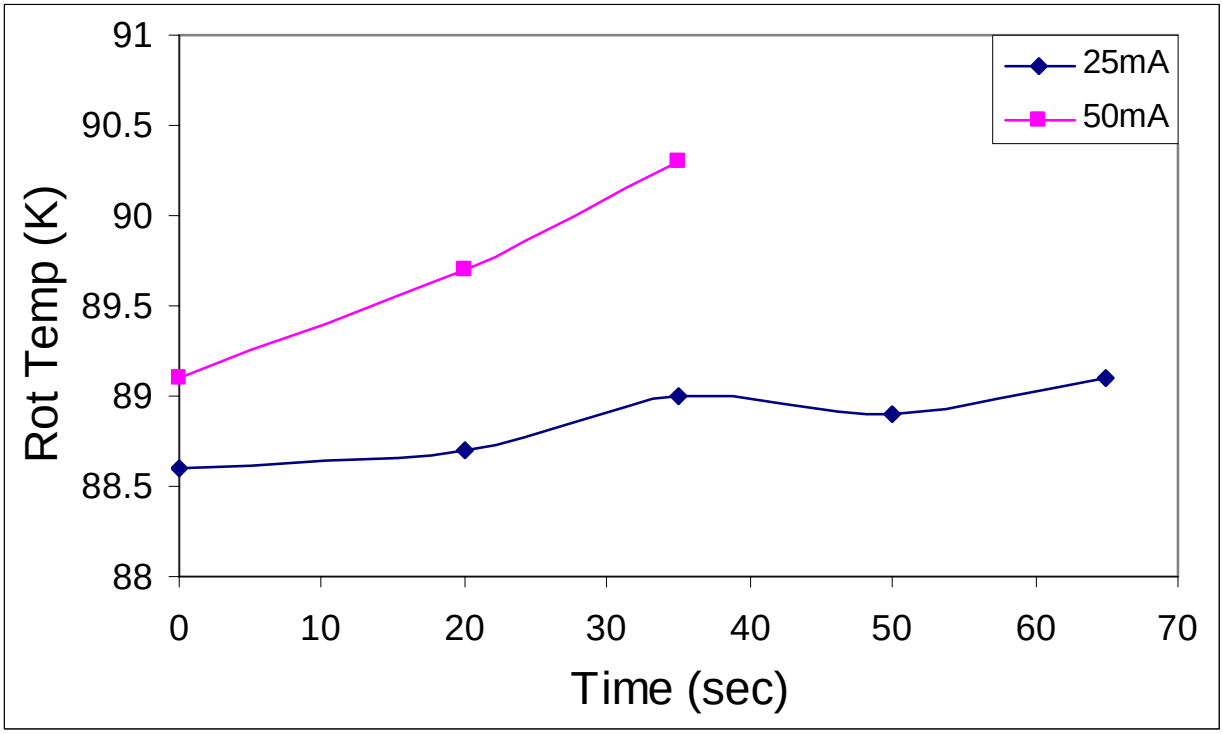

Figure 8. Time dependence on temperature in the free stream at the cathode for an elevation of 4.09 mm.

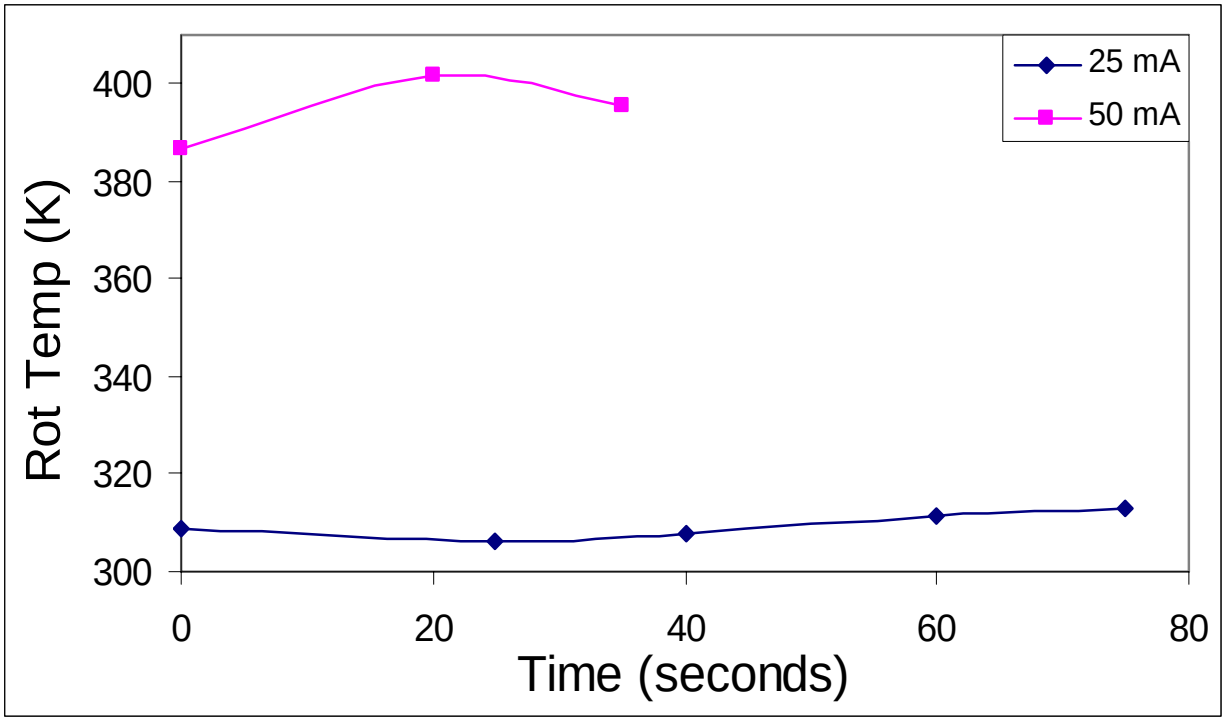

Figure 9. Time dependence on temperature in the boundary layer at the cathode for an elevation of 0.273 mm.

VI. Conclusion

Spatially resolved rotational temperatures have been obtained inside the boundary layer of a flat plate model with a surface plasma discharge in a Mach 5.1 air flow. The maximum temperature measured for both the 25mA case and 50mA case occurs over the cathode at an elevation of 0.546 mm. The maximum temperatures for these two different currents were 384 K and 301 K respectively. Because the temperature drops in both vertical directions from this maximum it can be conclude that heat is being convected into the surface of the plate for a period of time when the discharge is first turned on. This is a possible explanation for some trends seen in pitot and total lift measurements made in other work done by the authors. The temperature profile over the cathode shows a small temperature change across an oblique shock. The measured temperature change across the shock of 7 K does not agree with the calculated change of 18 K. The disagreement is believed to be caused by a weak signal in this region of the discharge and from reflected light. The temperature profile obtained for the anode shows a relatively constant temperature value of 299 K out to an elevation of 3 mm. This work also shows that the temperature of the gas above the cathode does change with time. This change with time diminishes at locations well above the copper electrode. This temporal dependence along with the negative temperature slope at the cathode surface indicates that the copper cathode is heating and thus reducing the amount of energy being dumped into the air flow, for a period of time, right above the model surface.

Acknowledgments

The authors would like to thank Dr. Charles DeJoseph for his time, expertise knowledge and eagerness to help us get this spectroscopic system working. Many informative discussions with him during the course of this work were invaluable. The authors would also like to that him for supplying his program N2SPECFIT and for loaning a tungsten filament spectral lamp to the project.

References

[1] Kimmel, R. L., "Aspects of Hypersonic Boundary Layer Transition Control", AIAA Paper 2003-0772, January 2003.

[2] Ganguly, B. N., Bletzinger, P., and Garscadden, A., "Shock Wave Damping and Dispersion in Non-equilibrium Low Pressure Argon Plasma," *Physical Letters*, Vol. 230, 1997, pp. 218.

[3] Shang, J. S., Canupp, P. W., and Gaitonde, D. V., "Computational Magneto-Aerodynamic Hypersonics," AIAA Paper 99-4903, November 1999.

[4] Shang, J., Gaitonde, D., Updike, G., "Simulating Magneto-Aerodynamic Actuator for Hypersonic Flow Control", AIAA paper 2004-2657, 35th AIAA Plasma Dynamics and Lasers Conference, Portland, Oregon, June 2004.

[5] Ganiev, Y., Gordeev, V., Krasilnikov, A., Lagutin, V., Otmennikov, V., and Panasenko, "Aerodynamic Drag Reduction by Plasma and Hot-Gas Injection", *J. Thermophysics and Heat Transfer*, Vol. 14, No. 1, 2000, pp. 10-17.

[6] Shang, J. S., "Plasma Injection for Hypersonic Blunt Body Drag Reduction", *AIAA J*, Vol. 40, No. 6, 2002, pp. 1178-1186.

[7] Girgis, I., Shneider, M., Macheret, S., Brown, G., and Miles, R. B., "Creation of Steering Moments in Supersonic Flow by Off-Axis Plasma Heat Addition," AIAA 2002-0129, January 14-17, 2002.

[8] Menart, J., Shang, J., Kimmel, R. L., and Hayes, J. R., "Effects of Magnetic Fields on Plasmas Generated in a Mach 5 Wind Tunnel," AIAA Paper 2003-4165, June 2003.

[9] Kimmel, R. L., Hayes, J. R., Menart, J. A., Shang, J., "Effect of Surface Plasma Discharges on Boundary Layers at Mach 5" AIAA Paper 2004-509, January 2004.

[10] Kimmel, R., Hayes, J., Menart, J., Shang, J., Henderson, S., "Measurements of a Transverse DC Discharge in a Mach 5 Flow", AIAA paper 2003-3855, 34th Plasmadynamics and Lasers Conference, Orlando, FL, June 2003.

[11] Williamson, J., DeJoseph, Jr, C., "Determination of Gas Temperature in an Open-Air Atmospheric Pressure Plasma Torch from Resolved Plasma Emission", *J. of Applied Physics*, Vol. 93, No. 4, 2003, pp. 1893-1898.

[12] Laux, C.O., Gessman, R.J., Kruger, C.H., Roux, F., Michaud, F., Davis, S.P., "Rotational Temperature Measurements in Air and Nitrogen Plasmas Using the First Negative System of N_2^+", *Journal of Quantitative Spectroscopy & Radiative Transfer*, Vol. 68, 2001, p. 473-482.

[13] Marr, G., *Plasma Spectroscopy* Elsevier Publishing Company, New York, 1968.

[14] Howatson, A., *An Introduction to Gas Discharges*, 2nd ed. Pergamon Press, New York, 1976.

[15] Shang, J.S., Kimmel, R., Hayes, J., and Tyler, C., "Performance of a Low-Density Hypersonic Magneto-Aerodynamic Facility", AIAA paper 03-329, January 2003.

[16] Herzberg, G., *Molecular Spectra and Molecular Structure I. Spectra of Diatomic Molecules*, 2nd ed. Van Nostrand Reinhold, New York, 1950.

[17] Kimmel, R. L., Hayes, J. R., Menart, J. A., Shang, J., "Effect of Magnetic Fields on Surface Plasma Discharges at Mach 5" AIAA Paper 2004-52661, July 2004.

[18] Menart, J, Stanfield, S., Shang, J., Kimmel, R., and Hayes, J, "Study of Plasma Electrode Arrangements for Optimum Lift in a Mach 5 Flow," AIAA 2006-1172, January 2006.